Lecture 2:

How to Design a Tokamak?

AP 4990y Seminar

Columbia University

Spring, 2011

Summary: ITER's Parameters

$$P_\alpha + P_{aux} + P_{oh} = 123 \text{ MW}$$

$$P_{rad} = P_{brem} + P_{cyc} + P_{line} = 48 \text{ MW}$$

Table 5.1. Nominal parameters of ITER-FEAT in inductive operation

Parameter	Units	Reference Q = 10	High Q, high P_{fus}
R/a	m/m	6.2 / 2.00	6.2 / 2.00
Volume	m^3	837	837
Surface	m^2	678	678
Sep.length	m	18.4	18.4
$S_{cross\text{-}sect.}$	m^2	21.9	21.9
B_T	T	5.3	5.3
I_p	MA	15.0	17.4
κ_x / δ_x		1.86 / 0.5	1.86 / 0.5
$\kappa_{95} / \delta_{95}$		1.7 / 0.35	1.7 / 0.35
$l_i(3)$		0.86	0.78
V_{loop}	mV	89	98
q_{95}		3.0	2.7
β_N		1.77	1.93
$<n_e>$	$10^{19}\,m^{-3}$	10.14	11.56
n/n_{GW}		0.85	0.84
$<T_i>$	keV	8.1	9.1
$<T_e>$	keV	8.9	9.9
$<\beta_T>$	%	2.5	3.2
β_p		0.67	0.62
$\boxed{P_\alpha}$	$\boxed{MW}$	$\boxed{82}$	120

Parameter	Units	Reference Q = 10	High Q, high P_{fus}
P_{aux}	MW	40	23
P_{ohm}	MW	1.3	1.7
P_{tot}	MW	123	144
P_{brem}	MW	21	29
P_{syn}	MW	8	10
P_{line}	MW	19	20
P_{rad}	MW	48	59
P_{fus}	MW	410	600
P_{sep}/P_{LH}	MW/ MW	75/48	84/53
$\boxed{Q}$		$\boxed{10}$	24
τ_E, s		3.7	4.1
W_{th}	MJ	325	408
W_{fast}	MJ	25	33
$H_{H\text{-}IPB98(y,2)}$		1.0	1.0
τ_α^*/τ_E		5.0	5.0
Z_{eff}		1.65	1.69
$f_{He,axis}$	%	4.1	5.9
$f_{Be,axis}$	%	2.0	2.0
$f_{C,axis}$	%	0.0	0.0
$f_{Ar,axis}$	%	0.12	0.11

$$\frac{W}{\tau_E} \sim 88 \text{ MW}$$

Performance calculations using the agreed physics guidelines yield a substantial operating window for $Q \geq 10$ inductive operation for the selected parameter set.

Outline

- Fusion power and Q
- Plasma operational limits
- Technology limits
- ITER's discharge targets

General tokamak design rules are now well-established

Reviews of Modern Physics, Vol. 66, No.3, July 1994

The physics of magnetic fusion reactors

John Sheffield
Oak Ridge National Laboratory, Oak Ridge, Tennessee 37831

During the past two decades there have been substantial advances in magnetic fusion research. On the experimental front, progress has been led by the mainline tokamaks, which have achieved reactor-level values of temperature and plasma pressure. Comparable progress, when allowance is made for their smaller programs, has been made in complementary configurations such as the stellarator, reversed-field pinch and field-reversed configuration. In this paper, the status of understanding of the physics of toroidal plasmas is reviewed. **It is shown how the physics performance, constrained by technological and economic realities, determines the form of reference toroidal reactors.** A comparative study of example reactors is not made, because the level of confidence in projections of their performance varies widely, reflecting the vastly different levels of support which each has received. **Success with the tokamak has led to the initiation of the International Thermonuclear Experimental Reactor project.** It is designed to produce 1500 MW of fusion power from a deuterium-tritium plasma for pulses of 1000 s or longer and to demonstrate the integration of the plasma and nuclear technologies needed for a demonstration reactor.

Basics

- Tokamak geometry (surface, volume, stability, field: B, a, $\kappa = b/a$, $\varepsilon = a/R$, ...)
- Plasma stability (pressure limits, density limits, current limits: q, β, β_N, n_G, ...)
- Nuclear reactivity (σ, ...)
- Power balance (thermal conduction, radiation: τ_E, χ, p_{brem}, p_{cyc}, ...)

D-T (^{6}Li) Fusion:
Easiest Fuel for Laboratory Power

$$3D + 3(^6Li) \rightarrow 6(^4He) + 3n + (10.5 \text{ MeV plasma}) + (56.4 \text{ MeV blanket})$$

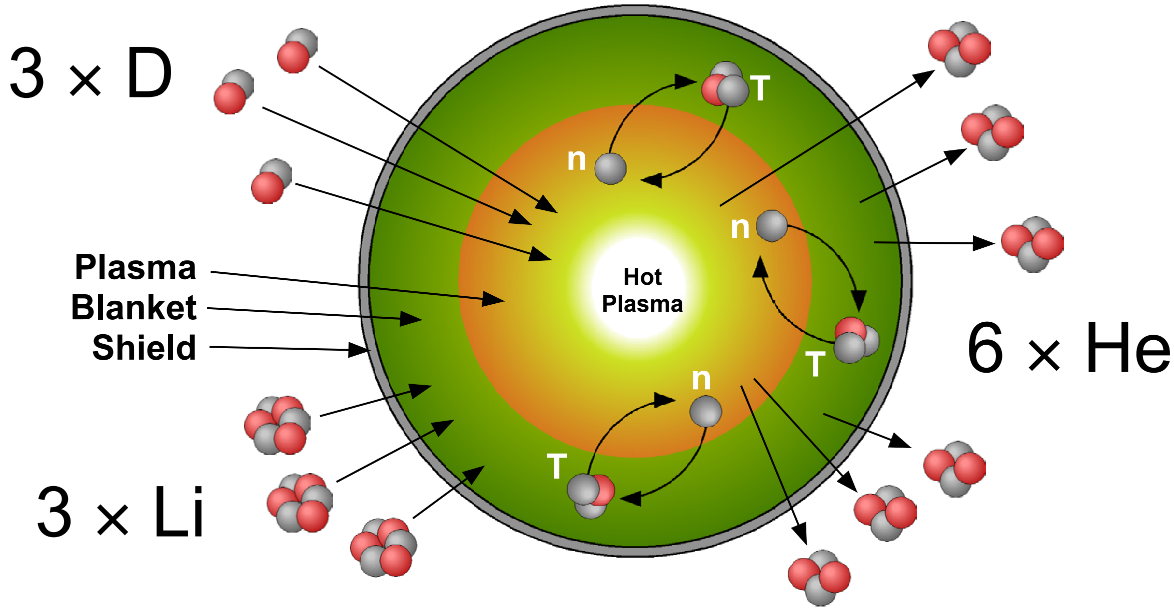

- D-T fusion has largest cross-section and lowest T ~ 170,000,000°.
- Tritium is created from ^{6}Li forming a **self-sufficient fuel cycle**. Practically no resource limit (10^{11} TW y D; 10^4(10^8) TW y ^{6}Li)!
- **Notice**: ~ 80% of energy as fast neutrons (~ 1.5 m shielding).

  ➠ the source of fusion's technology & materials challenge.

Other fuel cycles are possible, but *more challenging*, e.g.

D-D (^{3}He) Fusion

$$6D \rightarrow 2(^4He) + 3H + e^- + n + (41.5\ \mathrm{MeV\ plasma}) + (2.45\ \mathrm{MeV\ shield})$$

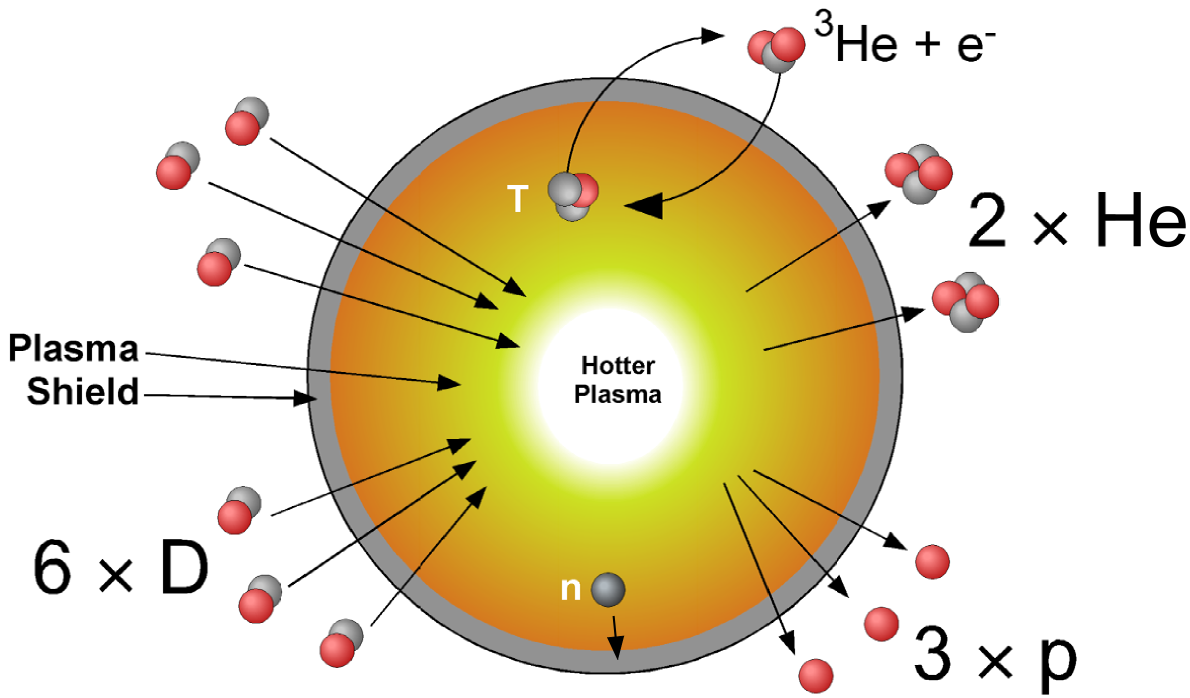

- Significantly reduced fast neutron flux!! Most energy to plasma and then first wall. Simplifies fusion component technologies.
- Next easiest fusion fuel cycle, but requires confinement ~25 times better than D-T(Li) **and** T extraction from plasma (*i.e.* only MFE).
- Equally challenging, but exciting, D-D options exist for IFE.

Self-Sustained Fusion Burn

- τ_E is plasma energy confinement time

- Lawson's condition:
  $\eta(P_{fus} + P_{aux}) > P_{aux}$

- $Q = P_{fus}/P_{aux}$

- Ignition: $Q \rightarrow \infty$, or …

$$\frac{W_p}{\tau_E} + P_{rad} = (\text{Charged Particle Fusion Power})$$

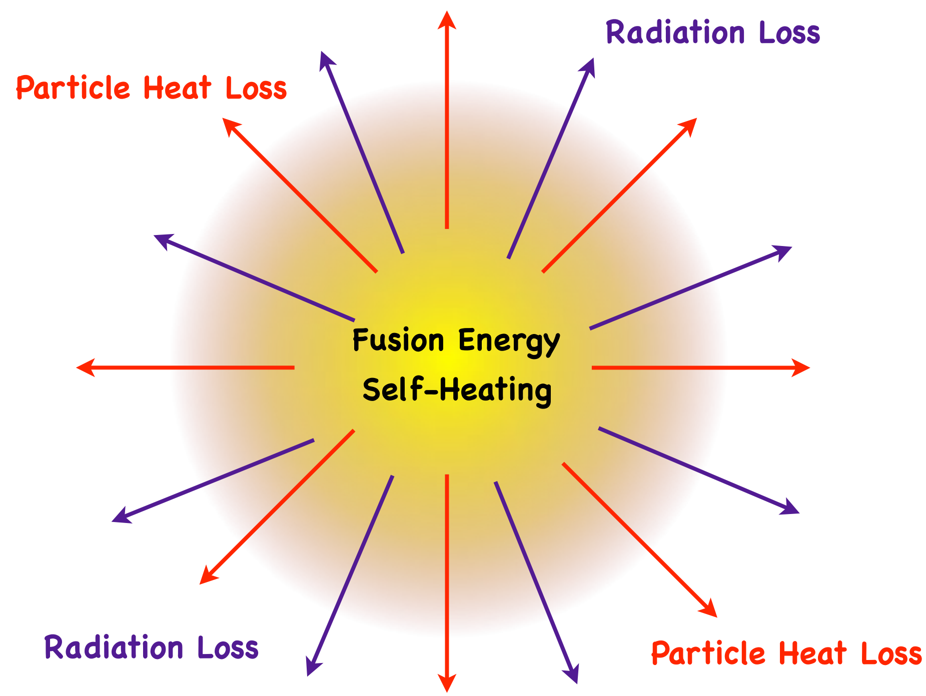

Neutrons escape and heat surrounding blanket

Basics: Geometry, τ_e, and β

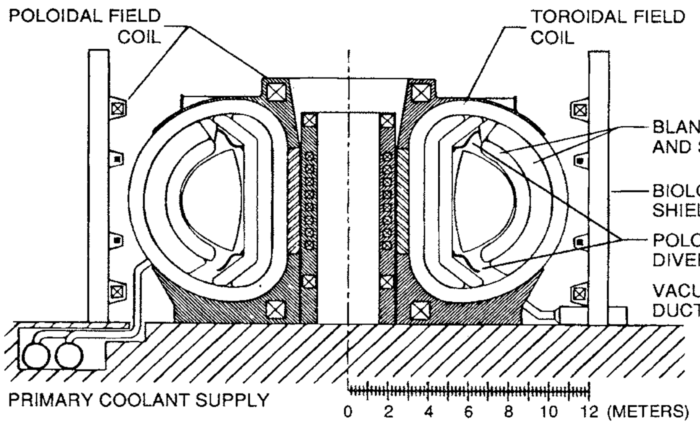

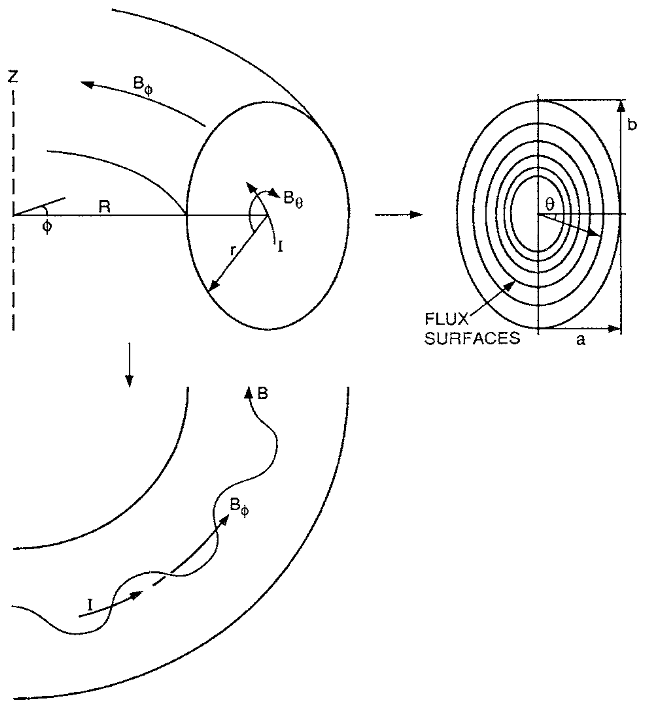

FIG. 2. Nested flux surfaces in a toroidal system.

Reviews of Modern Physics, Vol. 66, No.3, July 1994

Parameters of importance in characterizing the fusion plasma are the energy confinement time (τ_E), which equals the stored energy in the plasma (W) divided by the heat (P) leaving the plasma (excluding the neutrons),

$$\tau_E = \frac{W}{P}(s) \qquad (2.1)$$

and beta (β), which is the ratio of the kinetic pressure $(n_e kT_e + n_i kT_i + \Sigma n_z kT_z)$ of the plasma divided by the magnetic pressure,

$$\beta = \frac{(\text{pressure} \times 100)}{(B^2/2\mu_0)} \% \ . \qquad (2.2)$$

Basics: Fusion Reactivity

TABLE IV. Nuclear fusion reactions of greatest relevance to magnetic fusion. The final two quantities in each line refer to the total nuclear energy release in one reaction and to the energy release in the form of charged particles, respectively.

Reaction	Energy: Charged particle (MeV)	Energy: Total (MeV)	Energy: Total equivalent energy (kWh/g)
(1) $D+T \rightarrow {}^4He(3.52\ MeV)+n\ (14.06\ MeV)$	3.52	17.58	94,000
(2a) $D+D \rightarrow {}^3He(0.82\ MeV)+n\ (2.45\ MeV)$	0.82	3.27	22,000
(2b) $D+D \rightarrow T(1.01\ MeV)+p\ (3.03\ MeV)$	4.04	4.04	27,000
(3) $D+{}^3He \rightarrow {}^4He\ (3.67\ MeV)+p\ (14.67\ MeV)$	18.34	18.34	98,000

$$
\begin{aligned}
{}^6Li+n &= {}^4He+T+4.80\ \text{MeV}\ ,\\
{}^7Li+n &= {}^4He+T+n-2.47\ \text{MeV}\ .
\end{aligned}
\tag{2.3}
$$

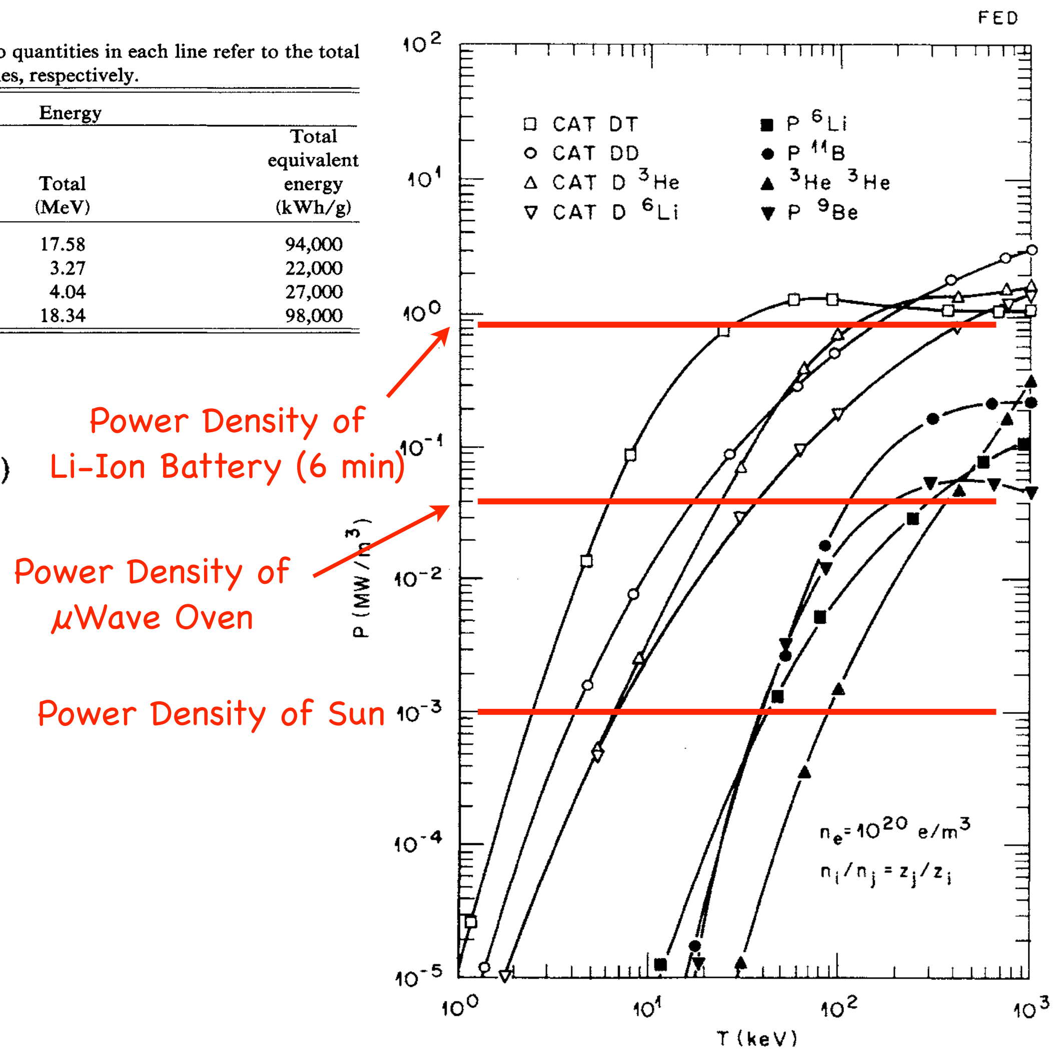

FIG. 3. Maximum charged-particle power density release vs temperature for the principal fusion fuels in thermalized plasmas at $n_e = 10^{20}\ m^{-3}$ and $n_i/n_j = Z_j/Z_i$. Power output scales as the square of the electron density (McNally, 1982).

Basics: Power Balance

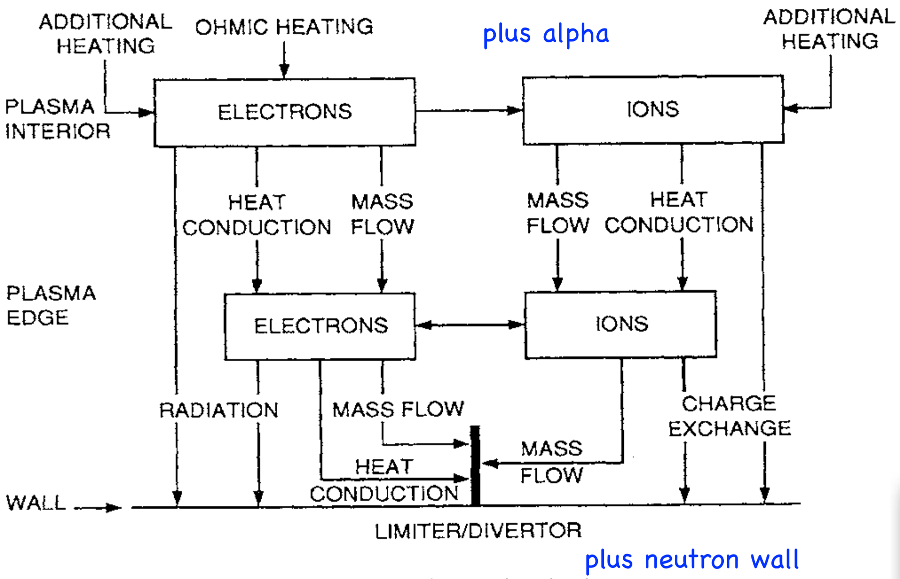

FIG. 4. Power flow in a typical toroidal plasma.

Profiles matter...

The power balance may be written separately for each species. For the electrons, a simplified power balance is

$$\frac{\partial}{\partial t}\left[\frac{3}{2}neT_e\right]=\frac{1}{r}\frac{\partial}{\partial r}r\left[n_e\chi_e\frac{e\partial T_e}{\partial r}+\frac{3}{2}D_A eT_e\frac{\partial n}{\partial r}\right]+p_\Omega$$
$$+p_{ie}-p_{LR}-p_{br}-p_S+p_r+p_{\alpha e}$$
$$+p_{ae}\ (\mathrm{W\,m^{-3}})\ . \qquad (2.11)$$

For the ions

$$\frac{\partial}{\partial t}\left[\frac{3}{2}n_i eT_i\right]=\frac{1}{r}\frac{\partial}{\partial r}r\left[n_i\chi_i\frac{e\partial T_i}{\partial t}+\frac{3}{2}D_A eT_i\frac{\partial n}{\partial r}\right]$$
$$+p_{ei}-p_{cx}+p_{ai}+p_{\alpha i}+p_{ai}\ (\mathrm{W\,m^{-3}})\ . \qquad (2.12)$$

Note that temperatures are given in electron volts. In

The bremsstrahlung power density (Rose and Clark, 1961, p. 232) for the range of $n(\mathrm{m}^{-3})$ and T_e (eV) values appropriate to D-T reactors is given approximately by

$$p_{\mathrm{br}}=1.7\times10^{-38}\zeta n_e^2 Z_{\mathrm{eff}} T_e^{0.5}(\mathrm{W\,m^{-3}})\ . \qquad (2.15a)$$

This represents the total emission at all wavelengths of the continuum from the free-free energy transitions of the (optically thin) plasma electrons. The Gaunt factor ζ corrects for electron-electron collisions and relativistic effects. For $1\ \mathrm{keV}<T_e<100\ \mathrm{keV}$, ζ varies from $1.2<\zeta<1.1$; see Ecker, 1972.

For a toroidal plasma, major radius R, minor radius in the median plane a, and ellipticity κ,

$$\tau_E=\tfrac{3}{2}2\pi^2Ra^2\kappa\frac{e\langle n_eT_e+n_iT_i\rangle}{P}\ (\mathrm{s})\ . \qquad (2.22)$$

For a plasma sustained by the fusion alpha power, and $T_{10C}<T_{10}<2T_{10C}$, a parabolic temperature profile ($\alpha_T=1$) and square-root parabolic density profile ($\alpha_T=0.5$), from Eq. (2.7) we have $T_{10C}=0.75$ and

$$P_\alpha=4.9\times10^{-42}\langle n_{DT}T_i^2\rangle^2Ra^2\kappa\ (\mathrm{W})\ , \qquad (2.23)$$

where n_{DT} is the density of deuterium plus tritium ions. Substituting for P_α in Eq. (2.22), with $T_e=T_i=T$, leads to a requirement for a self-sustaining pure D-T plasma ($n_e=n_i$)

$$\langle n_{\mathrm{DT}}T_i\rangle\tau_E\simeq1.93\times10^{24}\ (\mathrm{m^{-3}\ eV\,s})\ . \qquad (2.24)$$

For example, if $\langle n_{\mathrm{DT}}T_i\rangle=1.5\times10^{20}\ \mathrm{m}^{-3}\times10\ \mathrm{keV}$, we require $\tau_E=1.3$ s.

Basics: Power Balance

The line radiation is given by (Jensen *et al.*, 1977)

$$p_{LR} = \sum_z n_e n_z f(z) (\mathrm{W\,m^{-3}}) \,. \tag{2.14}$$

This is the dominant radiation term in present-day tokamaks (typically 20–40% of the power is radiated), and it is particularly important at the plasma edge. As shown in Fig. 5, $f(z)$ is a strongly increasing function of Z as the impurities become more massive. Consequently small amounts of heavy materials such as molybdenum and tungsten can have a disproportionately large effect.

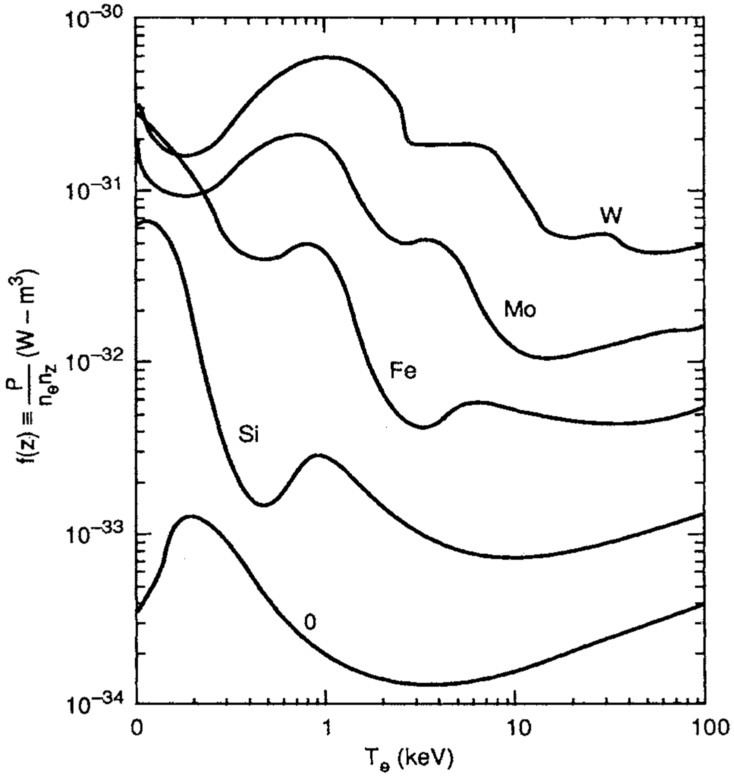

FIG. 5. Line radiation factor f (z) as a function of electron temperature for representative impurities (Jensen *et al.*, 1977).

Simple Fusion Power Conditions

$$f_\alpha P_{fus} + Paux = \frac{W}{\tau_E} + P_{brem} + P_{rad}$$

$$Q \equiv \frac{P_{fus}}{P_{aux}}$$

$$P_{fus} \propto P_{brem} \propto P_{rad} \propto n^2$$

$$nT\tau_E = \frac{n^2 V}{(f_\alpha + 1/Q)\,P_{fus} - P_{brem} - P_{rad}}$$

a function of T only

Simple Fusion Power Conditions

$$nT\tau_E = \frac{n^2 V}{(f_\alpha + 1/Q)\, P_{fus} - P_{brem} - P_{rad}}$$

$$nT\tau_E = 6.3 \times 10^{-6} \left(\frac{\beta}{\chi}\right) \times B^2 a^2$$

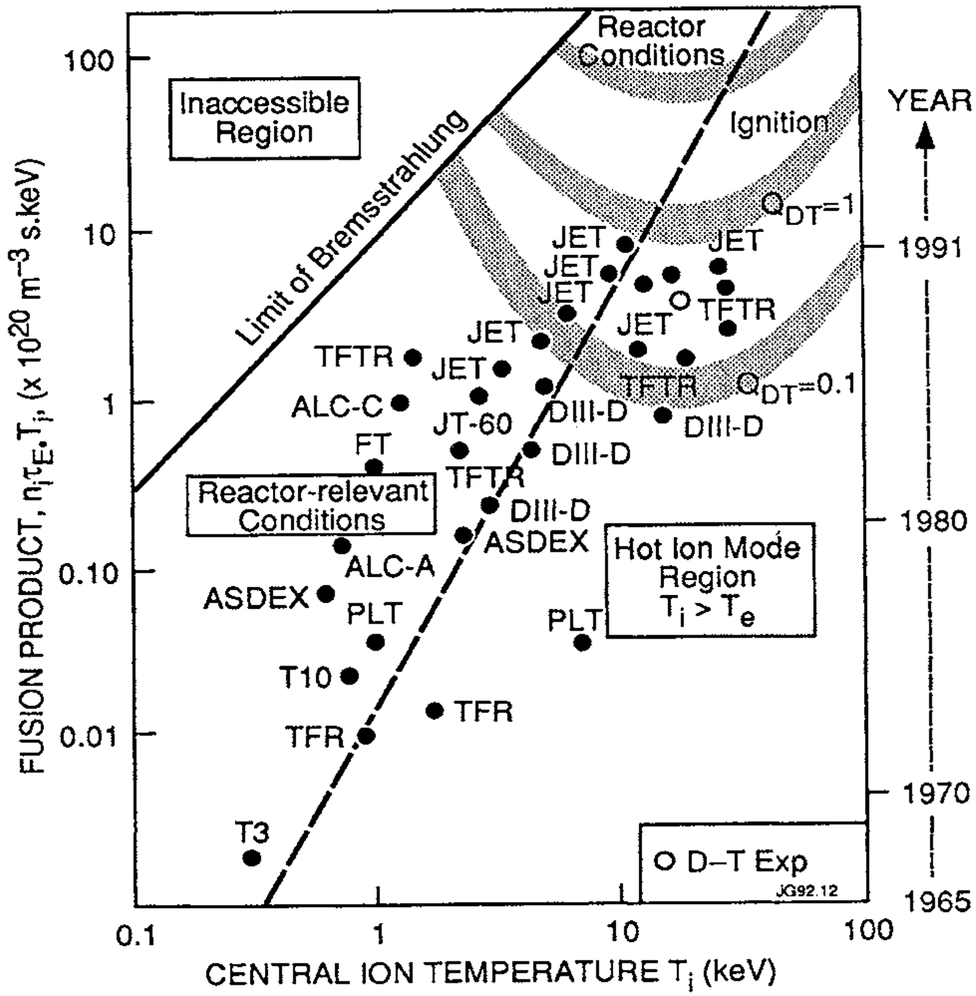

FIG. 31. Performance of tokamaks, JET Team, 1992.

Rev. Mod. Phys., Vol. 66, No. 3, July 1994

Confinement

5.3. Global scaling

Global scaling expressions for the energy confinement time (τ_E), or the stored energy (W), are powerful tools for predicting the confinement performance of burning plasmas. These expressions are described using engineering parameters, such as the major radius (R), minor radius (a) or inverse aspect ratio ($\varepsilon = a/R$), elongation (κ), toroidal magnetic field (B_t), plasma current (I_p), electron density (n_e), heating power (P) or loss power ($P_L \equiv P - dW/dt$) and ion mass number (M). One of the most reliable scaling expressions since 1998 for the ELMy H-mode thermal energy confinement time (τ_{th}) is the so-called IPB98(y,2) scaling [2]:

$$\tau_{th,98y2} = 0.0562 I_p^{0.93} B_t^{0.15} n_{19}^{0.41} P_L^{-0.69} R^{1.97} \varepsilon^{0.58} \kappa_a^{0.78} M^{0.19} \tag{30}$$

(in s, MA, T, 10^{19} m^{-3}, MW, m). The effective elongation is defined as $\kappa_a = S_c/\pi a^2$, where S_c is the plasma cross-sectional area. The interval estimation of τ_{th} in the ITER FDR with the use of such scaling expressions was studied in detail [2, 701]. Later estimation for the present ITER design using the extended database ITERH.DB3 showed a smaller interval of a 95% log-linear uncertainty (+14%/ − 13%) than that for ITER FDR (+25%/ − 20%) [704].

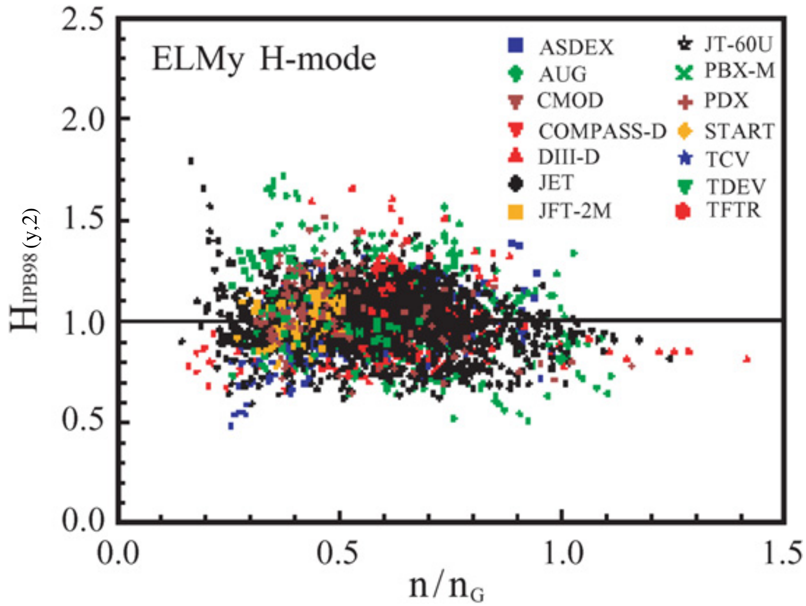

Figure 92. HH factor ($\equiv \tau_{th}/\tau_{th,98y2}$) versus n/n_G. Reprinted with permission from [698].

Nucl. Fusion **47** (2007) S18–S127

Simple Fusion Power Conditions

$$nT\tau_E = 6.3 \times 10^{-6} \left(\frac{\beta}{\chi}\right) \times B^2 a^2$$

$\beta/\chi_\perp \equiv \beta\, 2\tau_E/a^2$

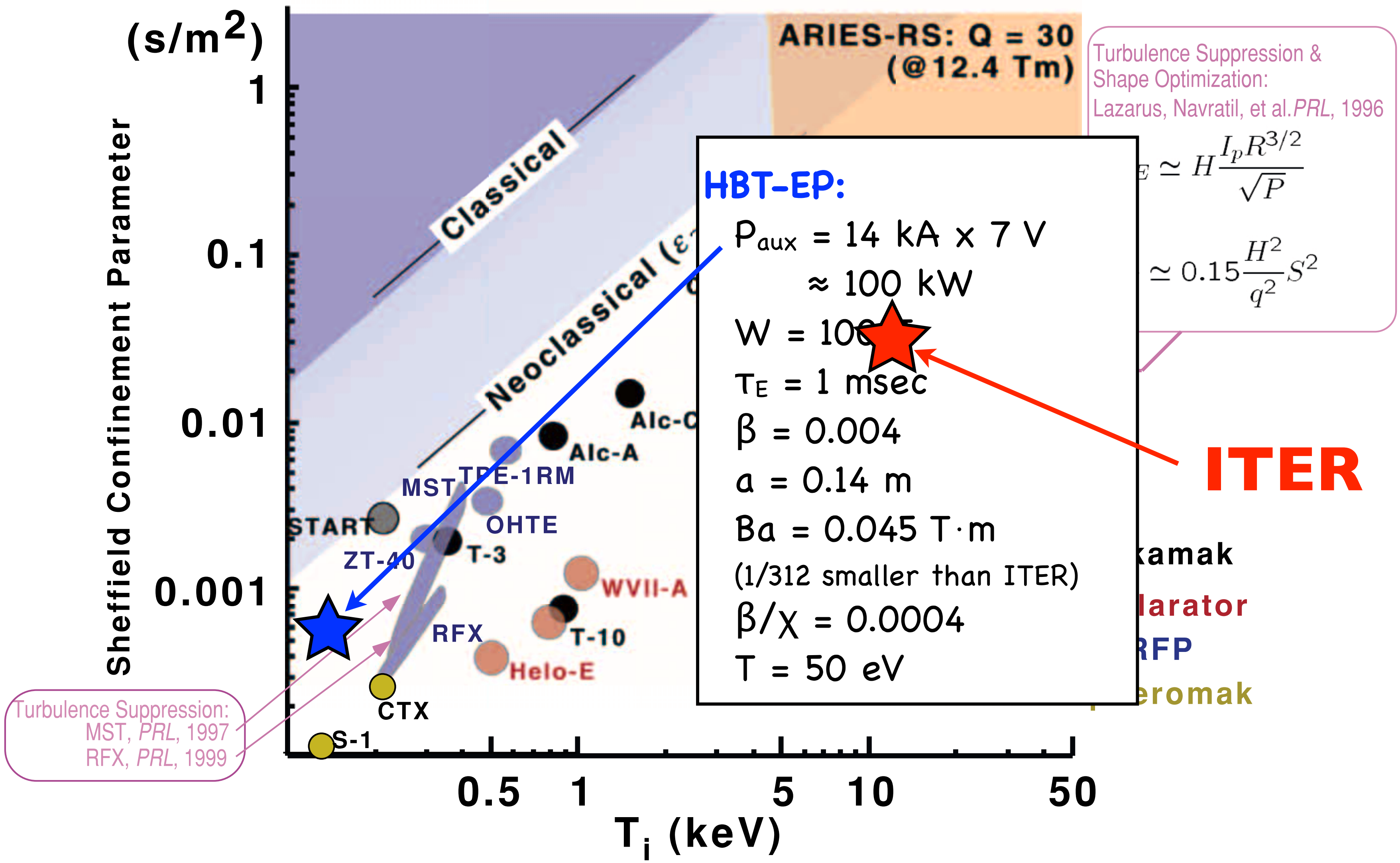

Summary: Fusion Power

- $T \approx 9$ keV
- $n \approx 10^{20}$ m^{-3}
- $\beta = 0.025$ (with $\beta_N = 1.8$)
- $B \approx 5.3$ T
- $\varepsilon = a/R = 0.32$ (with $\kappa = b/a = 1.7$)
- $a = 2$ m ($aB = 14$; with $I_p = 15$ MA and $q = 3.0$)
- $\tau_E = 3.7$ s (with $\beta/\chi \approx 0.027$)
- $Q \geq 10$

Summary: ITER's Parameters

$$P_\alpha + P_{aux} + P_{oh} = 123 \text{ MW}$$

$$P_{rad} = P_{brem} + P_{cyc} + P_{line} = 48 \text{ MW}$$

Table 5.1. Nominal parameters of ITER-FEAT in inductive operation

Parameter	Units	Reference Q = 10	High Q, high P_{fus}
R/a	m/m	6.2 / 2.00	6.2 / 2.00
Volume	m^3	837	837
Surface	m^2	678	678
Sep.length	m	18.4	18.4
$S_{cross\text{-}sect.}$	m^2	21.9	21.9
B_T	T	5.3	5.3
I_p	MA	15.0	17.4
κ_x / δ_x		1.86 / 0.5	1.86 / 0.5
$\kappa_{95} / \delta_{95}$		1.7 / 0.35	1.7 / 0.35
$l_i(3)$		0.86	0.78
V_{loop}	mV	89	98
q_{95}		3.0	2.7
β_N		1.77	1.93
$\langle n_e \rangle$	10^{19} m^{-3}	10.14	11.56
n/n_{GW}		0.85	0.84
$\langle T_i \rangle$	keV	8.1	9.1
$\langle T_e \rangle$	keV	8.9	9.9
$\langle \beta_T \rangle$	%	2.5	3.2
β_p		0.67	0.62
P_α	MW	82	120

Parameter	Units	Reference Q = 10	High Q, high P_{fus}
P_{aux}	MW	40	23
P_{ohm}	MW	1.3	1.7
P_{tot}	MW	123	144
P_{brem}	MW	21	29
P_{syn}	MW	8	10
P_{line}	MW	19	20
P_{rad}	MW	48	59
P_{fus}	MW	410	600
P_{sep}/P_{LH}	MW/ MW	75/48	84/53
Q		10	24
τ_E, s		3.7	4.1
W_{th}	MJ	325	408
W_{fast}	MJ	25	33
$H_{H\text{-}IPB98(y,2)}$		1.0	1.0
τ_α^* / τ_E		5.0	5.0
Z_{eff}		1.65	1.69
$f_{He,axis}$	%	4.1	5.9
$f_{Be,axis}$	%	2.0	2.0
$f_{C,axis}$	%	0.0	0.0
$f_{Ar,axis}$	%	0.12	0.11

$$\frac{W}{\tau_E} \sim 88 \text{ MW}$$

Performance calculations using the agreed physics guidelines yield a substantial operating window for Q ≥ 10 inductive operation for the selected parameter set.

Density, Beta, H-Mode Limits

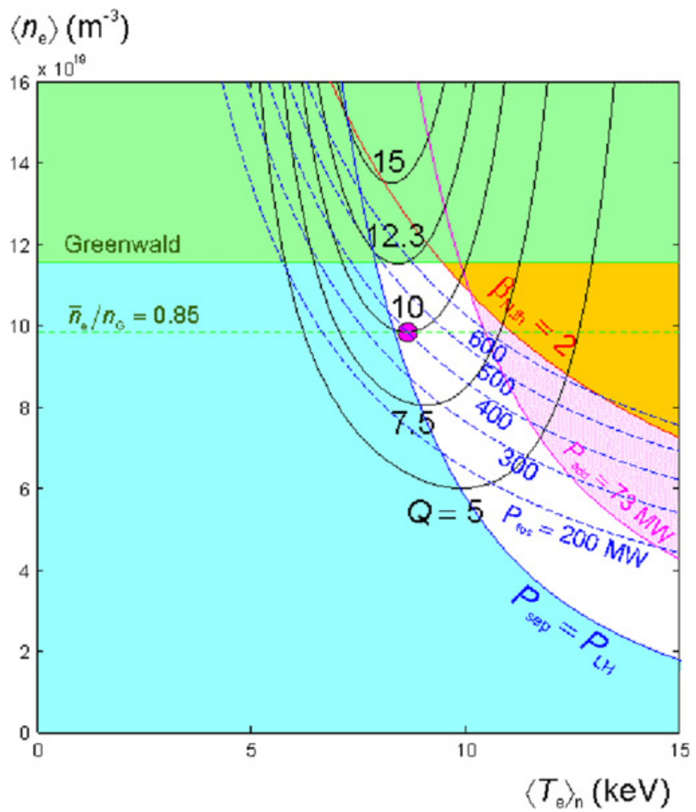

Figure 1. The operating space is shown on the basis of calculations using the HELIOS code for the baseline 15 MA, 5.3 T ELMy H-mode scenario. For reference, the baseline heating power is 73 MW. At an operating density of 0.85 of the Greenwald limit, the projected Q is 10 with 40 MW of heating power and $\tau_E = 3.8$ s The accessible operating regime in white is bounded by the estimated power required to achieve an H-mode, the Greenwald density and the available auxiliary heating power.

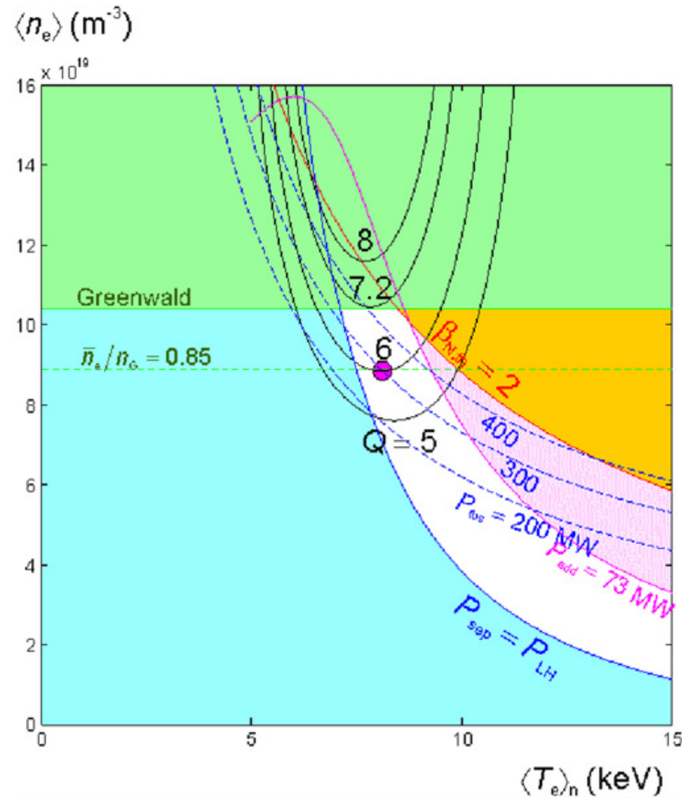

Figure 2. Operating scenario assuming a 10% reduction in toroidal field (4.77 T) and plasma current (13.5 MA) relative to figure 1. For the nominal operating point at 0.85 of the Greenwald density, $Q \sim 6$ and $\tau_E = 3.3$ s.

Nucl. Fusion **49** (2009) 065012

Density Limit

4.1.3. Understanding of density-limiting processes. There are several density limits in tokamaks [1, 431]. Two of them, i.e. the H-mode density limit associated with a back transition from H- to L-mode and the ultimate L-mode density limit related to plasma disruption are the most important for reactor like devices. The figure of merit for the L-mode density limit is the Greenwald density [1, 431],

$$n_G = \frac{I_p}{\pi a^2} \equiv 1.59 g \frac{B_t}{q_{95} R} \ (10^{20}\,\mathrm{m}^{-3},\ \mathrm{MA},\ \mathrm{T},\ \mathrm{m}), \quad (12)$$

where $g = q_{95}/q_{cyl}$ is the plasma shaping factor with $q_{cyl} = 5a^2 B_t/(R I_p)$. Typically, at operation in the Type I ELMy H-mode with gas puff fuelling, an increase in density above some limit leads to a transition from Type I to Type III ELMs accompanied with reduction of the stored plasma energy by 15–40% [503]. A further increase in the gas fuelling rate leads to a back transition to the L-mode, correlated with complete divertor detachment and/or divertor/X-point MARFE formation [1]. At even higher fuelling rates, the L-mode density limit disruption occurs, terminating the discharge.

E.J. Doyle *et al*

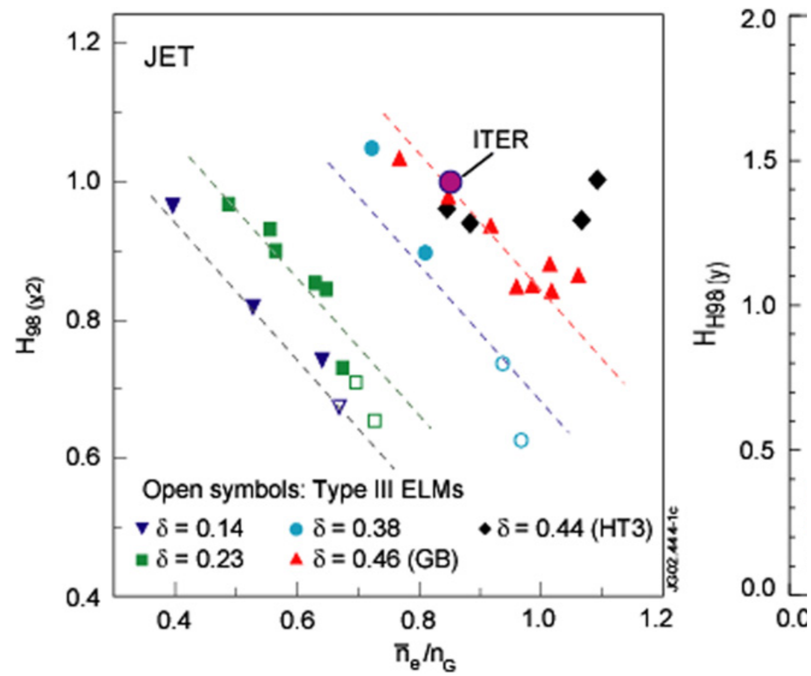

Figure 55. Confinement enhancement factors relative to the empirical H-mode c
triangularities δ. (Left) JET. Reprinted with permission from [370]. (Right) ASD

β Limit

Stability of high beta tokamak plasmas*

E. J. Strait†
General Atomics, P.O. Box 85608, San Diego, California 9218

(Received 5 November 1993; accepted 3 January 1994)

Stability at high beta (the ratio of plasma pressure to n
requirement for a compact, economically attractive fusio
large tokamak experiments, where the best performan
rather than by energy transport. The past decade has see
of the stability of high beta tokamak plasmas, as well a
beta. Ideal magnetohydrodynamic (MHD) theory has b
the stability limits, and the scaling of maximum stable b
predicted by Troyon and others has been confirmed
$\beta_{max} \approx 3.5$ (%-m-T/MA) I/aB (where I is the plasma
the toroidal field). The instabilities which are predic
experimentally, in good agreement with theoretical pred
modes and short-wavelength ballooning instabilities. A
stability have opened several paths to higher values of be
approaching the limits of axisymmetric stability, has all
reached in agreement with Troyon scaling. Recent
modeling have shown that the beta limit depends on the
profiles, and modification of the current density to creat
beta values up to $6I/aB$ to be achieved experimentally.
explore both local and global access to the predicted sec
with the potential for very high values of $\beta/(I/aB)$. Pre
wall stabilization and radio-frequency (RF) current prc
improvements in beta through passive and active cc
understanding of high beta stability and the applica
experiments and future fusion devices hold the potenti
plasmas at high beta with good confinement.

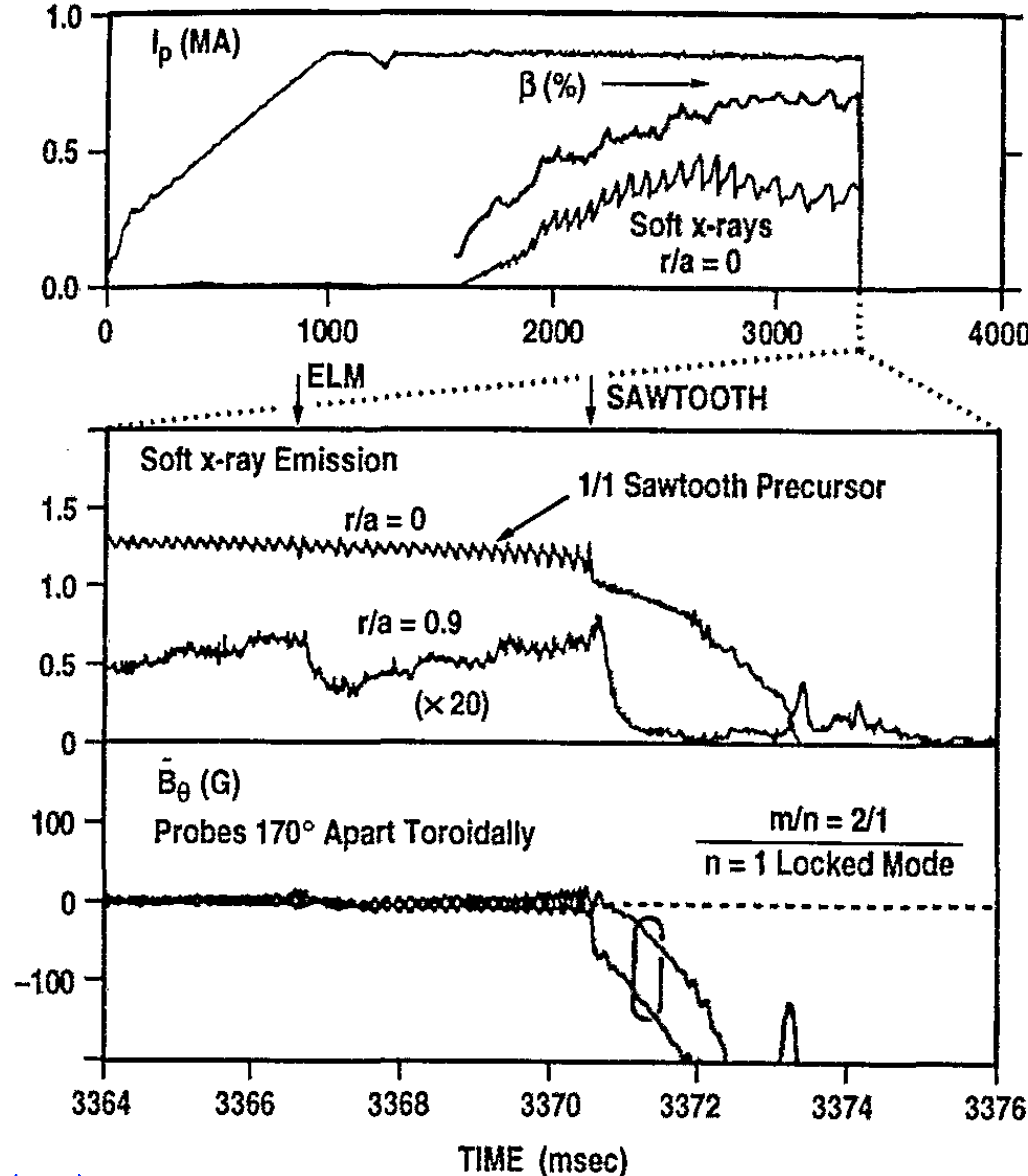

FIG. 4. Time evolution of an ideal $n=1$ kink mode disruption at high beta ($\beta_N=3.5$) in DIII-D (Ref. 49).

Strait. "Stability of high beta tokamak plasmas". Phys Plasmas (1994) vol. 1 pp. 1415

β Limit

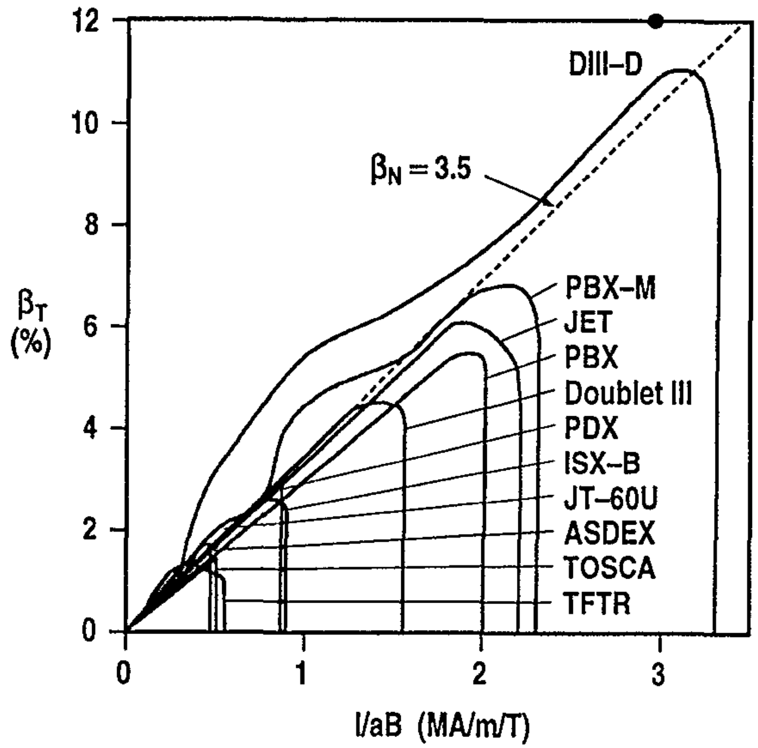

FIG. 2. Comparison of experimental beta limits to Troyon scaling, showing the operational envelopes for several tokamaks.

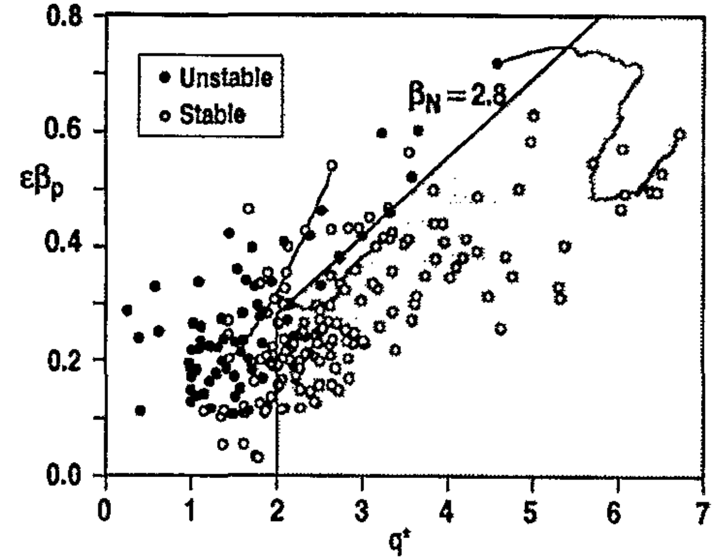

FIG. 3. Operational limits for HBT. Open circles indicate stable discharges; closed circles indicate transient, unstable cases with a growing $n=1$ kink instability. The $q=2$ limit and $\beta_N=2.8$ (Troyon) limit are shown (Ref. 46).

Strait. "Stability of high beta tokamak plasmas". Phys Plasmas (1994) vol. 1 pp. 1415

β and Density Limit

$$\langle\beta\rangle \sim 10^{-2}\beta_N\left(\frac{I\ (\mathrm{MA})}{aB}\right)$$

$$\langle n\rangle \sim 10^{20}\mathrm{m}^{-3}\,n_G\left(\frac{I\ (\mathrm{MA})}{\pi a^2}\right)$$

$$\langle T\rangle \propto \frac{\langle\beta\rangle}{\langle n\rangle} = 0.4\ \mathrm{keV}\,(aB)\frac{\beta_N}{n_G}$$

≈ 10 keV (ITER) and 30 eV (HBT-EP)

Neoclassical Tearing Modes (NTMs)

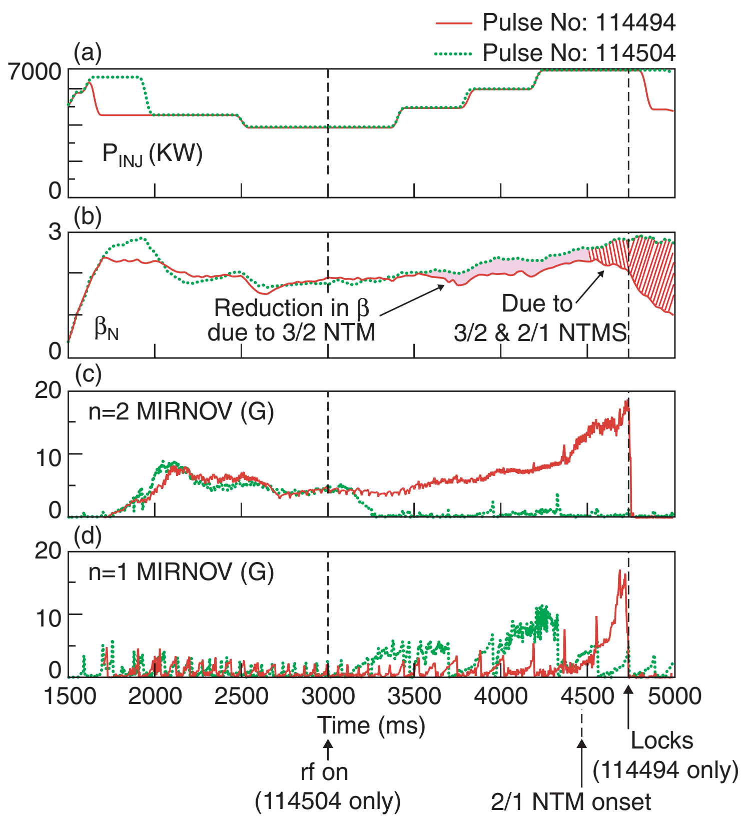

Figure 2. DIII–D discharges with (114504, dotted lines) and without (114494, solid lines) ECCD suppression of an $m/n = 3/2$ neoclassical tearing mode. (*a*) Neutral beam power, (*b*) β_N, (*c*) $n = 2$ Mirnov $|\tilde{B}_\theta|$, (*d*) $n = 1$ Mirnov $|\tilde{B}_\theta|$. The degradation in energy confinement due to the NTM from 3/2 and 2/1 NTMs can be seen in the effect on β_N.

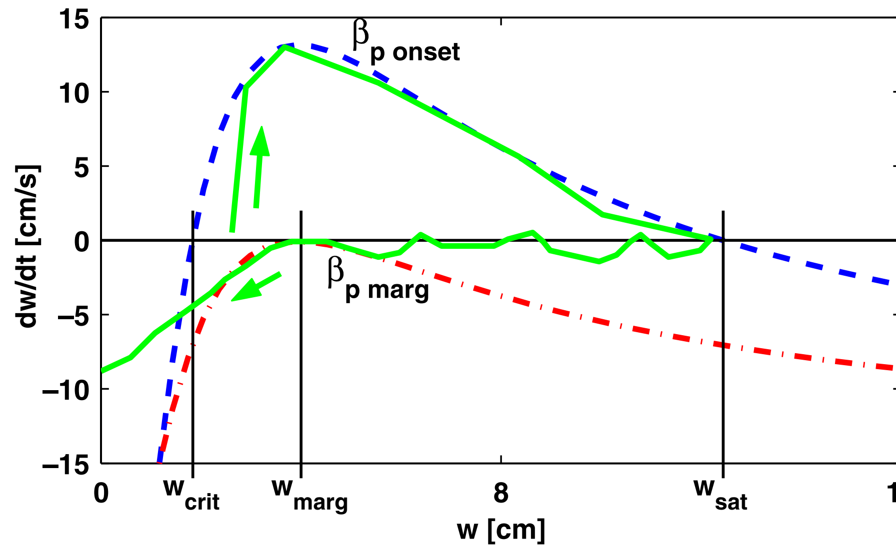

Figure 3. Sketch of the time evolution of the island growth rate as given by equation (6) at the onset of the NTM when the critical seed island size (W_{crit}) is exceeded and an NTM forms at $\beta_{p,onset}$. A slow decrease in beta from $\beta_{p,onset}$ to $\beta_{p,marg}$ (when $\max(dW/dt) = 0$) is assumed, as in power ramp-down experiments, such that $dW/dt \approx 0$ (reproduced from [54] 'Marginal β-limit for neoclassical tearing modes in JET H-mode discharges').

$$\frac{\tau_R}{r_s}\frac{dW}{dt} = r_s\Delta'(W) + r_s\beta_p(\Delta'_{BS} - \Delta'_{GGJ} - \Delta'_{pol}) + r_s\Delta'_{CD}. \tag{6}$$

Nucl. Fusion **47** (2007) S128–S202

ITER (Fusion) Requires Large Size (aB) and High Power

- Very strong magnets and large forces
- Very high power flux to limiters

Magnets

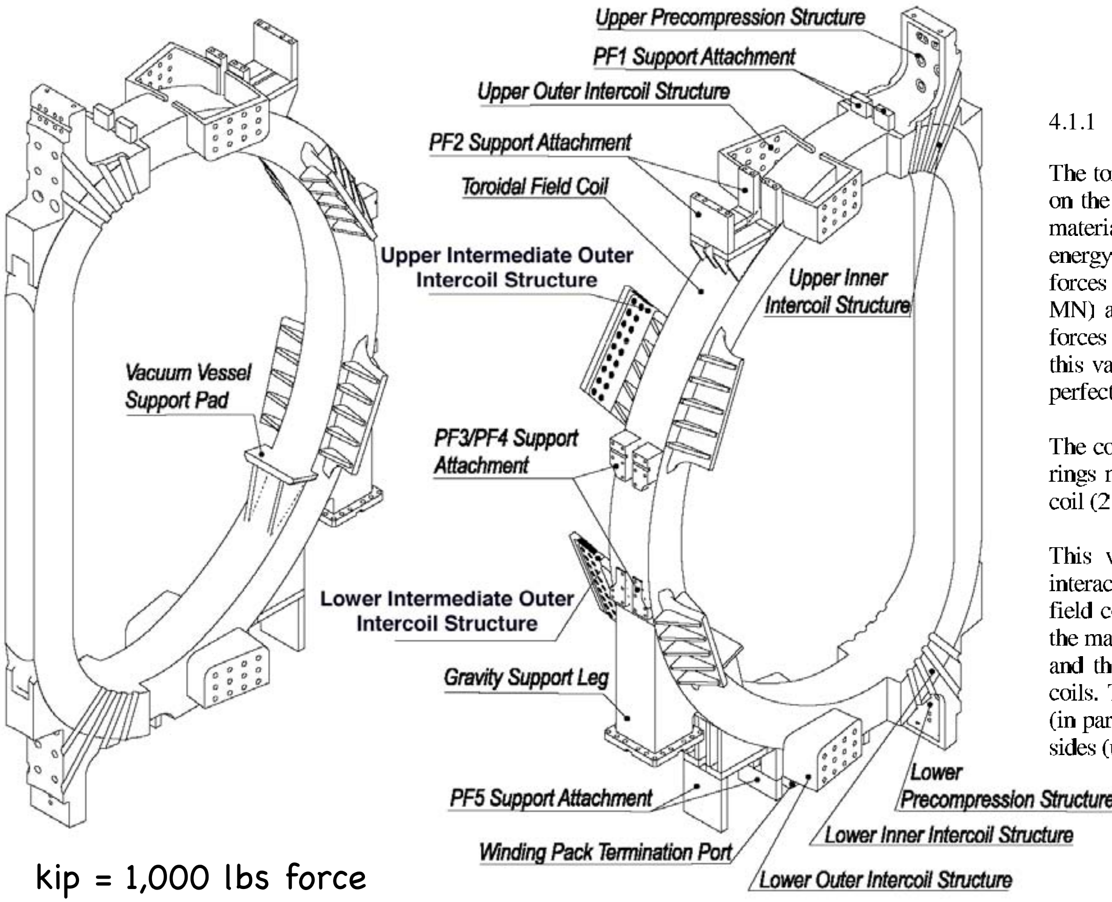

4.1.1 Toroidal Field Coils

The toroidal magnetic field value on the plasma axis is 5.3T, which leads to a maximum field on the conductor ≤ 12 T. Because of this high field value, Nb_3Sn is used as superconducting material, cooled at 4.5K by a flow of supercritical helium at ~ 0.6 MPa. The total magnetic energy in the toroidal field is around 40 GJ, the confinement of which leads to significant forces on each coil restrained by a thick steel case to resist circumferential tension (≈ 100 MN) and by constructing a vault with the inboard legs of all 18 coils (the large centripetal forces are due to the 1/R variation of the toroidal field). The compressive stress levels inside this vault are large, and therefore the side surfaces of each coil should match one another as perfectly as possible.

The coils are connected together (Figure 4.1-2) by bolted structures, and by two compression rings made of unidirectional glass fibres, that provide an initial inward radial force on each coil (2 x 30 MN).

This very robust assembly is provided mainly to resist the toroidal forces induced by interaction of the TF coil current with the transverse poloidal field from plasma and poloidal field coils. These forces produce a distribution of torque around the TF coil proportional to the magnetic flux crossing unit length (the net torque is thus 0). These local forces are pulsed, and therefore mechanical fatigue is a concern for the highly stressed structural steel of the coils. These forces, due to the highly shaped plasma, are largest across the inboard coil legs (in particular at their lower curved region) where they are resisted by the friction between coil sides (under high compression) and by specific keys.

kip = 1,000 lbs force

0.1 x GWB

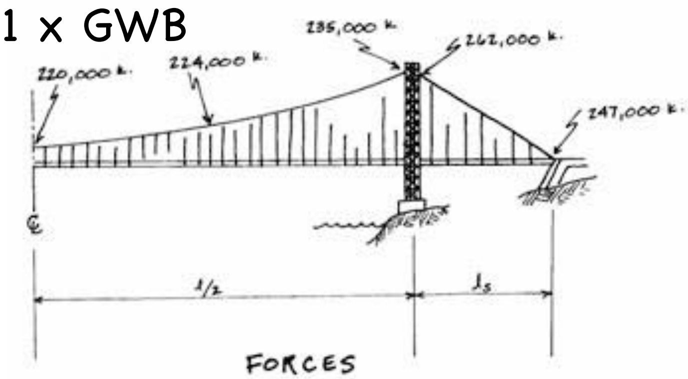

22 million pounds tension

Divertors

2 m

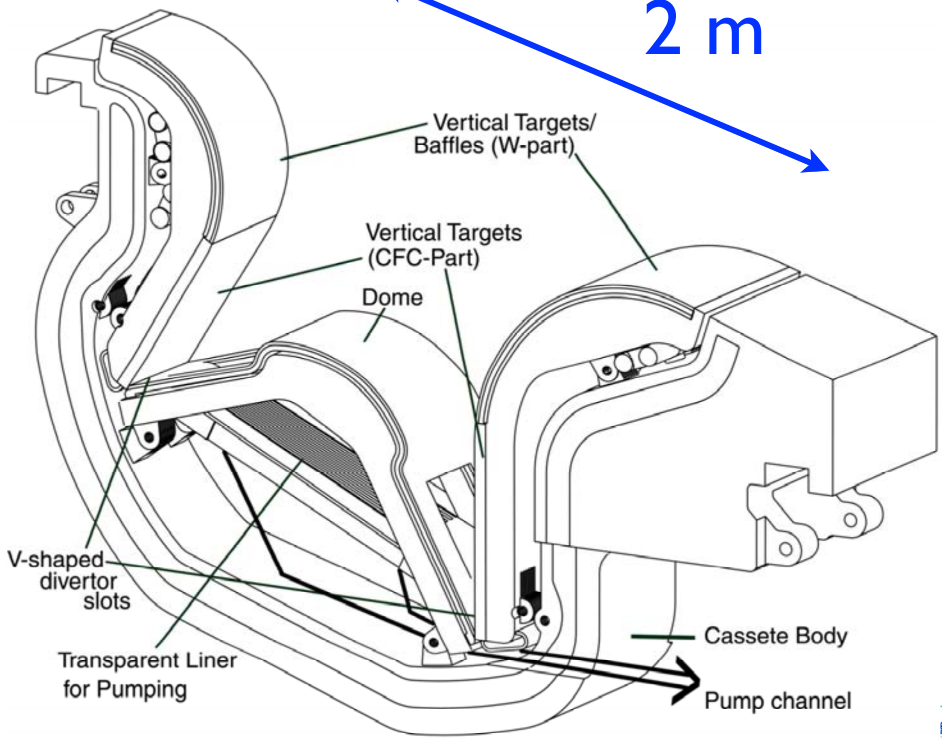

Figure 4.2-2
Divertor Cassette

4.2.5 In-vessel Component Water Cooling

Each divertor cassette is separately cooled by water, with feeder pipes connecting to the manifold outside the vessel and cryostat. Groups of two or three blanket modules are similarly fed by separate pipes installed on the plasma side of the inner shell of the vacuum vessel. This arrangement leads to handling a large number of small size pipes, but (e.g. by “spiking” specific coolant channels with tracer elements) allows the identification of possible modules or cassettes leaking water, from tests outside the cryostat, a crucial procedure to be able to rapidly localise the leaks in vacuum.

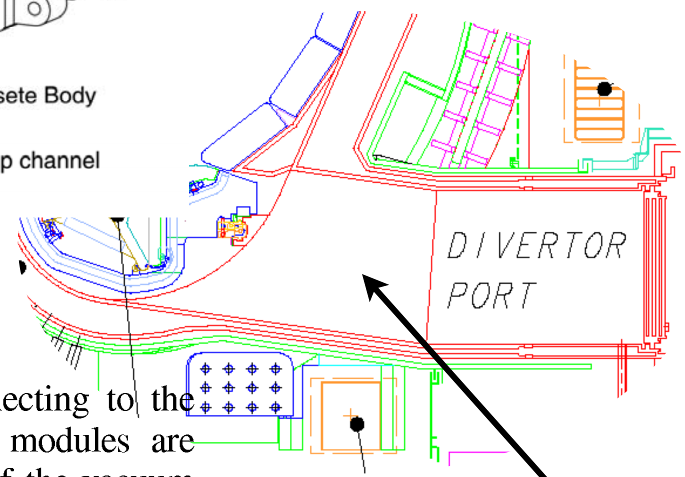

Cryopumping for
500 s...
300,000 Torr l/s

Thin SOL & Elms

Chapter 4: Power and particle control

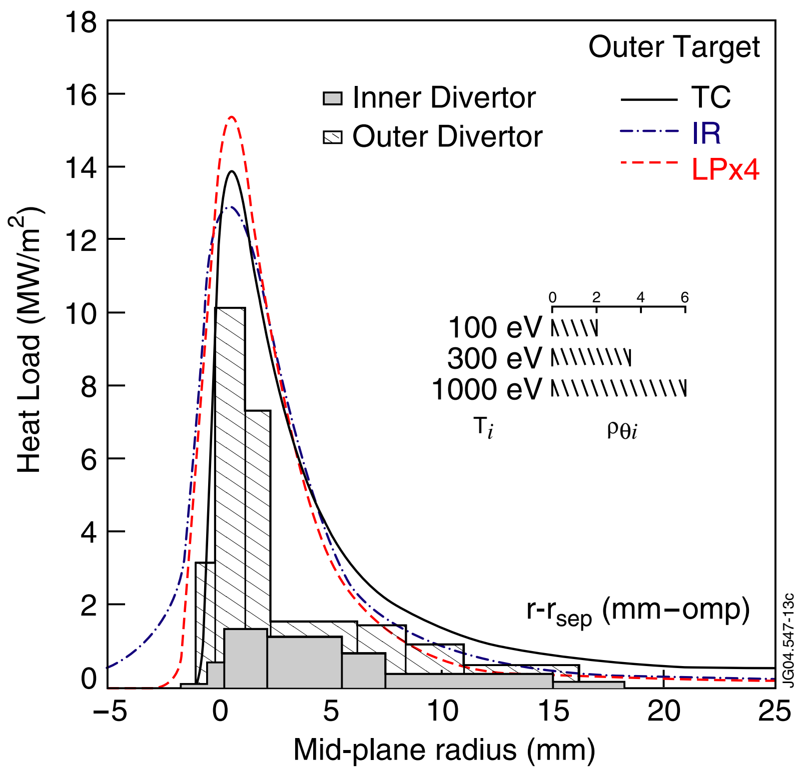

Figure 1. Comparison of ELM-averaged IR, LP (inter-ELM) and TC (histograms, ELM-averaged) derived heat flux profiles on the JET outer divertor target for a plasma with 16 MW NBI, 2.5 MA/2.4 T and ion $B \times \nabla B$ towards the X-point. The scale of the electron heat flux (LP) is four times smaller in the high power case. Also shown are the profiles obtained for a 12 MW Type I H-mode (same field and current), using the shot-by-shot TC method (——). For comparison the poloidal gyro-radius at the outer mid-plane is shown for three values of the ion energy [21].

Chapter 4: Power and particle control

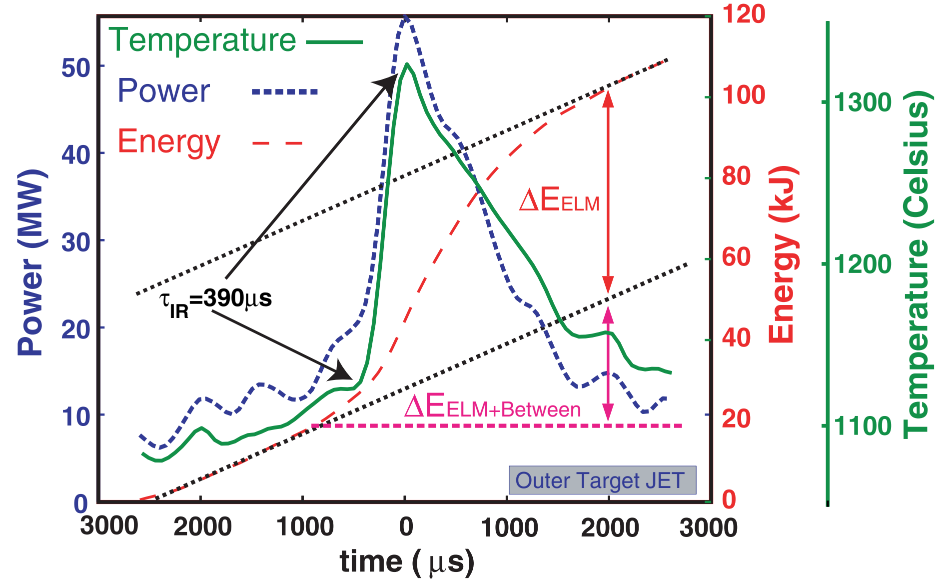

Figure 8. Temporal evolution of the divertor surface temperature, deposited ELM power and energy onto the JET outboard divertor target for a typical Type I ELM [162].

Summary

- Fusion cross-sections determine the scale ($Ba \sim 14$ T·m) of burning plasma experiment
- $\beta/\chi \sim 0.027$ s/m^2 is based upon existing data
- β_N and n_G are conservative limits
- ITER's size scale necessitates state-of-the art engineering and technology.